LETTERS

Geological record of fluid flow and seismogenesis along an erosive subducting plate boundary

Paola Vannucchi[1], Francesca Remitti[2] & Giuseppe Bettelli[2]

Tectonic erosion of the overriding plate by the downgoing slab is believed to occur at half the Earth's subduction zones[1,2]. *In situ* investigation of the geological processes at active erosive margins is extremely difficult owing to the deep marine environment and the net loss of forearc crust to deeper levels in the subduction zone. Until now, a fossil erosive subduction channel—the shear zone marking the plate boundary[3]—has not been recognized in the field, so that seismic observations have provided the only information on plate boundary processes at erosive margins. Here we show that a fossil erosive margin is preserved in the Northern Apennines of Italy. It formed during the Tertiary transition from oceanic subduction to continental collision, and was preserved by the late deactivation and fossilization of the plate boundary. The outcropping erosive subduction channel is ~500 m thick. It is representative of the first 5 km of depth, with its deeper portions reaching ~150 °C. The fossil zone records several surprises. Two décollements were simultaneously active at the top and base of the subduction channel. Both deeper basal erosion and near-surface frontal erosion occurred. At shallow depths extension was a key deformation component within this erosive convergent plate boundary, and slip occurred without an observable fluid pressure cycle. At depths greater than about 3 km a fluid cycle is clearly shown by the development of veins and the alternation of fast (co-seismic) and slow (inter-seismic) slip. In the deepest portions of the outcropping subduction channel, extension is finally overprinted by compressional structures. In modern subduction zones the onset of seismic activity is believed to occur at ~150 °C, but in the fossil channel the onset occurred at cooler palaeo-temperatures.

Tectonic erosion is commonly assumed to take place within the upper plate landward of a frontal prism (Fig. 1a, b). The frontal prism at the toe of erosive subduction zones is rarely static. Originally thought to be an accretionary structure composed of sediments scraped from the incoming plate, it is now known that it is often a contractional structure composed of disaggregated material from the upper plate[4]. Deeper, tectonic erosion has been assumed to occur by high-friction mechanical coupling between the plates, inducing pervasive abrasion of the overriding plate[5,6] (Fig. 1a). In contrast, alternative hypotheses[7] and geophysical data suggest that subducting plate boundaries are fluid-rich[8,9]. Fluids may play a key part in affecting the frictional behaviour of faults[10,11] and in weakening the upper plate[4] (Fig. 1b).

Here we discuss observations from a newly recognized fossil erosive subduction channel active from late Eocene (~35 Myr ago) to middle Miocene (~11 Myr ago). These outcrops in the Northern Apennines of Italy (Fig. 2) are a unique example of an erosive subduction zone where preservation occurred because of the deactivation of the plate boundary (followed by exhumation and partial erosion) (Supplementary Note 1). Here we focus on the implications of this preserved geological record for details of erosive plate boundary structures and deformation processes.

The Apennine subduction channel is ~500 m thick and extends 200 km along-strike. It is formally known among Apennine geologists as the Sestola–Vidiciatico unit (SVU) (Fig. 2). At present, the SVU is sandwiched between the overlying Late Cretaceous/early Eocene accretionary prism (that is, the frontal European plate margin) and the underlying fold-and-thrust belt formed by Adriatic continental units. The subduction channel is made of a melange formed by tectonically and gravitationally reworked blocks of (1) the previous, Late Cretaceous/early Eocene accretionary prism, (2) debris flow deposits of the frontal prism, and (3) late Eocene/middle Miocene slope sediments deposited on top of the frontal prism[12] (Supplementary Note 2).

Thus the SVU represents a large shear zone between the overriding European plate and the underlying Adriatic plate, and it contains material coming only from the overriding plate, consistent with it being the shallow portion of an erosive subduction channel.

The poorly exposed upper tectonic contact of the SVU with the overlying fossil accretionary prism maintains a planar geometry at the regional scale, indicating that, although active, it has never been involved in the collisional fold-and-thrust architecture[13] (Fig. 2).

The well-exposed lower tectonic contact of the SVU on the foredeep sequences has a map-scale ramp-and-flat geometry[14] with the deepest outcropping portion involved in a series of kilometre-size thrusts and folds[13] (Figs 2, 3). The development of these shortening structures indicates the deactivation of the deeper portion of the basal décollement, whereas its shallower portion and the upper décollement were still active and responsible for the northeastward migration of the upper plate on top of the foredeep turbidites. We propose that deactivation of the deeper portion of the lower décollement is associated with a period of uplift during the early–middle Miocene boundary[15,16] that reflects crustal thickening by tectonic underplating of subducted material along the landward portion of the forearc at the same time as tectonic erosion was occurring close to the trench.

The presence of a roof and a basal décollement that simultaneously cut through the margin toe implies that they were able to incorporate intact slices of the frontal prism through a process of frontal tectonic erosion (Fig. 1c). This ongoing process progressively incorporated younger slope sediment and older parts of the overlying former accretionary prism.

Our study of the internal fabric of the subduction channel concentrated on the slope sediment blocks that do not contain the deformation imprint of any previous subduction phase. In the shallower portion of the subduction channel (less than ~3 km, based on the thickness of overlying sediments) these blocks record a pervasive deformation represented by sets of extensional shear fractures

[1]Dipartimento di Scienze della Terra, Università di Firenze, Via La Pira, 4, 50121 Firenze, Italy. [2]Dipartimento di Scienze della Terra, Università di Modena e Reggio Emilia, Largo S. Eufemia, 19, 41100 Modena, Italy.

(Fig. 3a) with minor contraction. Veining is absent. The fractures tend to die out along the contact with the already lithified pieces of the melange, indicating strong differences in mechanical behaviour between its components. The field data sets (Fig. 2) consistently show two conjugate and contemporaneous sets of gently dipping normal faults producing a three-dimensional (3D) geometry comparable to a flattened bipyramid (Fig. 3a). The bipyramids have their minor axis nearly parallel to the vertical direction where the faces show angles of 110–120°. The observed polymodal fracture pattern can be explained by a 3D brittle shear failure criterion[17,18]. However, this model fails to explain the development of two conjugate shear planes that are inclined at an angle >45° to the axis of maximum compressive stress, although a high angle is consistent with unconsolidated, hence very weak sediments. Apparently, this shallower portion accommodated strain through contemporaneous failure and compaction, the latter inducing flattening of the bipyramids.

We speculate that consolidation is difficult in a fluid-rich, low-permeability environment. Strengthening may occur through the development of high fracture densities that act as dewatering conduits[19]. The sediment volume then becomes separated into multiple discontinuous elements along the subduction channel. The deformation zone remains weak because its elements are continually cut by new fracture episodes as soon as they develop strain hardening. In addition, this shallower portion of the subduction channel, in spite of being a mega-shear zone in a compressive geodynamic environment, experienced simultaneous extension.

In the intermediate portion of the subduction channel, evidence of extension is also found where diffuse deformation evolves into concentrated shear. Here, normal faults formed with a spacing of ~10 m. They cut the basal décollement (Fig. 3b), often reusing pre-existing discontinuities, and they are cut by successive slip along the décollement. These structures intersect all the SVU components, indicating that by this stage the unit had a homogeneous mechanical behaviour. Clay mineral assemblages are seen to have undergone a partial to total smectite-to-illite transformation; this reaction implies an important fluid source (Fig. 1d). Discrete normal faults also developed in the

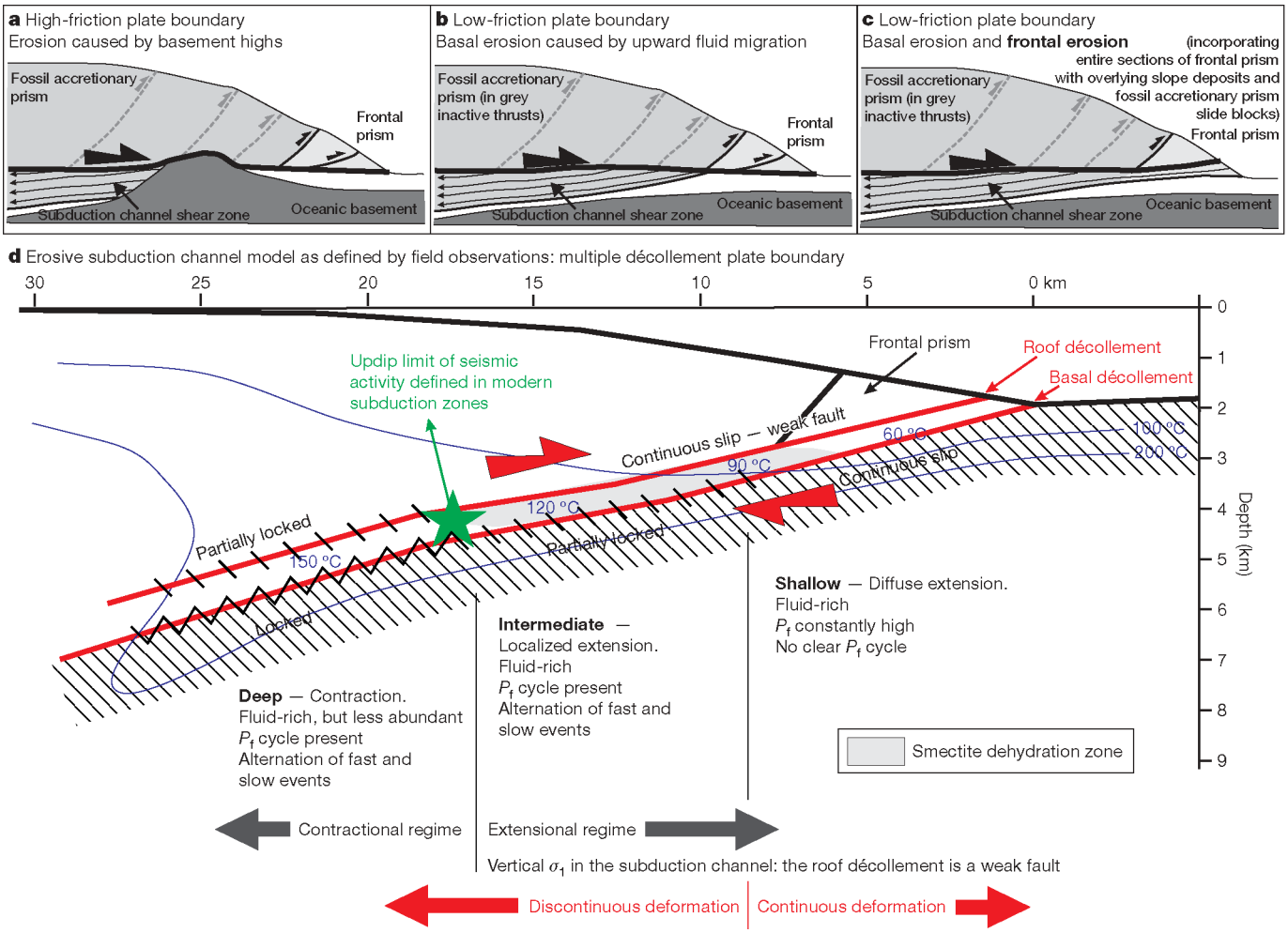

Figure 1 | Schematic models of tectonic erosion. Arrows in the subduction channel indicate relative velocities removing material from the base of the overriding plate. **a**, The model used in refs 5, 6 and 27: high-friction décollement steps up into a fossil accretionary prism as a result of subduction of the basement high (inactive thrusts are shown in grey). The subduction channel incorporates material ahead of the basement high. **b**, The model used in ref. 4: low-friction décollement steps up as a result of high fluid pressure causing hydrofracturing and weakening at the base of the overriding plate. Tectonic erosion is localized landward of the frontal prism and the subduction channel incorporates blocks from the overriding plate. **c**, The model proposed in this paper: a low-friction décollement cuts through the margin toe and incorporates in the subduction channel debris material from the frontal prism and associated slope sediments as well as material from the base of the overriding plate. **d**, Schematic model of the Apennine subduction channel. Thermal constraints and seismic activity[28,29] are taken from the well-studied erosive Costa Rica margin. The SVU subduction channel indicates an abundance of fluids throughout its length, but with different fluid sources. In the shallow portion the unconsolidated state of the sediment suggests that the predominant fluid source was sedimentary water. In the intermediate portion, consolidation suggests that sedimentary water is no longer the predominant fluid source. Clay mineral assemblages record a partial to total smectite-to-illite transformation, so that here this reaction could have been the predominant fluid source[25]. For the basal décollement, evidence for discontinuous slip occurs at shallower depth than for the roof décollement, and it migrates landward as well as upward. Evidence for discontinuous slip is even present in the extensional strain regime of the subduction channel.

footwall foredeep turbidites, but these footwall faults are widely spaced and only through the first 10 m below the contact. Faults are 10 cm to 1 m thick and permeated by dense arrays of extensional calcite veins. Each fault accommodates centimetre-scale displacement that is reached after a great number of repeated smaller events. The internal structure of the veins indicates that the faults were initially characterized by dilational stepovers, which allowed the opening of void spaces, and crack-and-seal fabric and pressure-solution testify to cyclical fluid pressure rises and drops that were followed by mineral precipitation, and then a new loading phase (Fig. 3b). Brecciation of both the previously precipitated calcite and the wall rocks is present within the dilational jogs, suggesting a triggering mechanism related to local fluid pressure drops, that is, implosions.

Strain concentration within the subduction channel developed in a generally extensional regime, associated with a fluid pressure cycle[20,21]. Two competing processes accommodate this deformation: (1) calcite veins and implosion breccias indicating relatively fast events and stress drop, and (2) slower pressure-solution.

In the deeper portion of the outcropping subduction channel extensional structures are finally overprinted by contractional structures. Here clay mineral assemblages, fluid inclusions, reflectance of organic matter[22], and fission tracks[23] all indicate that the sediment reached ~150 °C, corresponding to a depth of ~5 km. In modern subduction zones, 150 °C is often thought to be a key threshold temperature marking the updip limit of seismogenesis[24,25]. The involvement of the basal décollement in the fold-and-thrust deformation indicates locking, although fluid circulation was still active as shown by vein development (Fig. 3c).

Focusing on the relationship between the onset of shear concentration and the seismic cycle, the SVU points to a key role for episodes

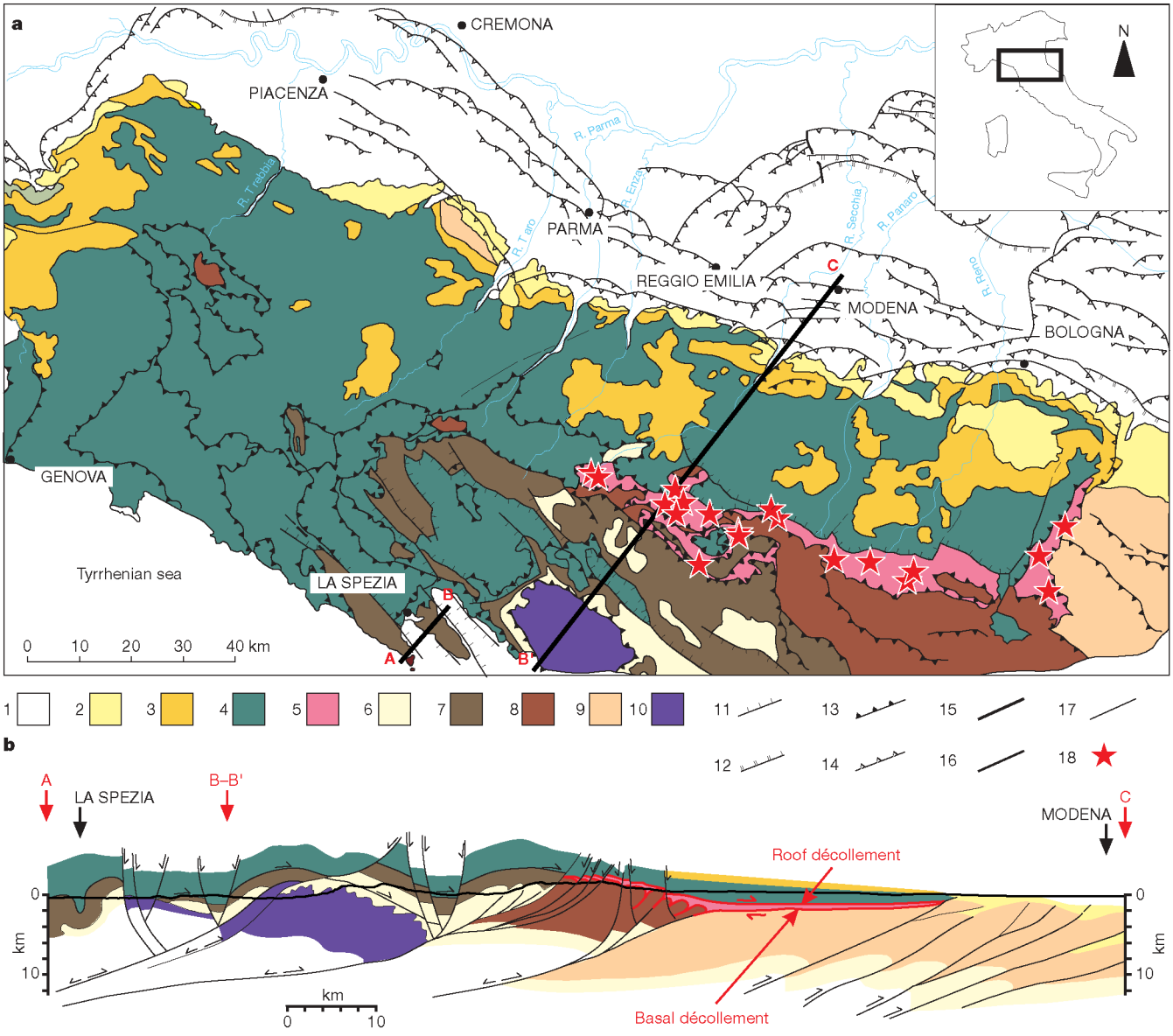

Figure 2 | Geological setting of the Northern Apennines. a, Schematic geological map with its geographic location shown in the inset. Key: (1) Quaternary deposits; (2) late Miocene–Pleistocene marine deposits; (3) Forearc slope deposits; (4) Oceanic units of the Late Cretaceous/early Eocene accretionary prism (European plate); (5) Sestola–Vidiciatico tectonic unit (subduction channel); (6) Mesozoic carbonate units of the Adria plate; (7) late Oligocene/early Miocene (Aquitanian) trench turbitites of the Adria plate; (8) early Miocene (Aquitanian–Burdigalian) foredeep turbidites of the Adria plate; (9) middle Miocene/late Miocene (Langhian–Messinian) foredeep turbidites of the Adria plate; (10) metamorphic continental units of the Adria plate; (11) normal faults; (12) normal faults (subsurface); (13) thrust faults and overthrusts; (14) thrust faults (subsurface); (15) strike-slip faults; (16) high-angle faults of unknown displacement (subsurface); (17) lithological boundaries; (18) location of detailed studied structural sections. **b**, Geological cross-section as marked on map (A–C). The thickness of the SVU is about 500 m, slightly decreasing towards the northeast.

Figure 3 | Photographs of mesoscopic structures characterizing the Apennine fossil subduction channel. **a**, Shallow portion: (1) and (2), extensional shear fractures cutting through the blocks of lower slope marls at the metre-scale and at the centimetre-scale. Red arrows indicate the fractures. The shear fractures occur at all scales of observations in the same geometry, until the complete loss of the sedimentary fabric. (3) Equal-angle, lower-hemisphere stereographic projection of extensional shear fractures and associated striae at the site shown in (1). (4) Three-dimensional bipyramidal element defined by the extensional shear fractures. **b**, Intermediate portion: (5) Basal décollement separating the SVU/subduction channel from the underlying foredeep turbidites of the Adria plate. Here the basal décollement (~5 cm thick) is separating the debris flow component of the subduction channel from the foredeep turbidites. The basal décollement is cut by high-angle normal faults filled by calcite veins and with displacements of about 1–2 m towards the southwest. In general the main direction of movement recorded by the normal faults is parallel to the direction of the Apennine tectonic transport, northeast, but southwest, northwest and southeast displacements are also present. (6) Close up of the shear zone marking the basal décollement; (7) dilational jog along the basal décollement; (8) thin section of a calcite vein showing crack-and-seal fabric (parallel polars). **c**, Deep portion: (9) basal décollement involved in an anticline fold indicating shortening and locking; (10) the basal décollement, which now has a vertical orientation as a consequence of its involvement in an anticline, shows extensional calcite veins associated with the shortening stage of the basal décollement.

of extensional strain, where recurrent normal faulting creates a structural environment in which hydrofracturing can occur at relatively low values of $\lambda_v = P_f/\sigma_v$ (where P_f is fluid pressure and σ_v is overburden pressure)[26]. In this system we envisage conditions of anomalous high sediment strengthening relative to depth of the subduction channel.

The geological record within the fossil SVU subduction channel provides the following constraints on the tectonics and fluid flow at erosive subduction margins. (1) Two décollements were simultaneously active during plate convergence. They show differing down-dip mechanical slip behaviour and fluid flow. The presence of extensional shear strain in the channel and in foredeep turbidites indicates that the décollements were able to transmit lithostatic loads. This implies their weak nature until at least intermediate (~3 km) depths where the basal décollement became partially locked. At ~5 km depths, the basal décollement became fully locked, but the roof décollement was still able to transmit lithostatic load to the intermediate portion of the channel and became partially locked only in the deeper portion (Fig. 1d). (2) Both deeper basal erosion and near surface frontal erosion occurred. Frontal erosion has not yet been recognized at modern subducting margins, but may provide a key to interpret seismic images. (3) At shallow to intermediate depths, transient phases of extension with a large pure-shear component are a key mode of deformation within this convergent plate boundary. (4) At shallow depths (less than ~3 km), slip occurred without an observable fluid pressure cycle. We believe that this happened because the rock was too soft to let fluid pressure build up. Somewhat deeper in the subduction channel, as rocks acquired more strength, a fluid cycle is clearly shown by the development of veins. This fluid cycle records alternation of fast (co-seismic) and slow (inter-seismic) slip. Even deeper there is no evidence for convergence-linked extension, but the same fast and slow slip events are indicated within the subduction channel. (5) This subduction channel records the same 150 °C temperature that correlates with the updip limit of seismogenesis at modern subduction zones. Here the aseismic–seismic transition may correspond to the onset of the fluid pressure cycle in the extensional regime at temperatures even lower than 150 °C, with 150 °C marking the transition from extensional to compressional shear. This conjecture will be testable at modern subduction zones by drilling currently planned as part of the Integrated Ocean Drilling Program.

Received 15 June; accepted 12 November 2007.

1. Clift, P. & Vannucchi, P. Controls on tectonic accretion versus erosion in subduction zones: Implications for the origin and recycling of the continental crust. *Rev. Geophys.* **42,** RG2001, doi:10.1029/2003RG000127 (2004).
2. von Huene, R. & Scholl, D. W. Observations at convergent margins concerning sediment subduction, subduction erosion, and the growth of continental-crust. *Rev. Geophys.* **29,** 279–316 (1991).
3. Cloos, M. & Shreve, R. L. Subduction-channel model of prism accretion, mélange formation, sediment subduction, and subduction erosion at convergent plate margins: 1. Background and description. *Pure Appl. Geophys.* **128,** 455–500 (1988).
4. von Huene, R., Ranero, C. R. & Vannucchi, P. Generic model of subduction erosion. *Geology* **32,** 913–916 (2004).
5. Hilde, T. W. C. Sediment subduction versus accretion around the Pacific. *Tectonophysics* **99,** 381–397 (1983).
6. Dominguez, S., Malavieille, J. & Lallemand, S. E. Deformation of accretionary wedges in response to seamount subduction: Insights from sandbox experiments. *Tectonics* **19,** 182–196 (2000).
7. Le Pichon, X., Henry, P. & Lallemant, S. Accretion and erosion in subduction zones: The role of fluids. *Annu. Rev. Earth Planet. Sci.* **21,** 307–331 (1993).
8. Bilek, S. L. & Lay, T. Rigidity variations with depth along interplate megathrust faults in subduction zones. *Nature* **400,** 443–446 (1999).
9. Sage, F., Collot, J. Y. & Ranero, C. R. Interplate patchiness and subduction–erosion mechanisms: Evidence from depth-migrated seismic images at the central Ecuador convergent margin. *Geology* **34,** 997–1000 (2006).
10. Sibson, R. H. Frictional constraints on thrust, wrench and normal faults. *Nature* **249,** 542–544 (1974).
11. Segall, P. & Rice, J. R. Dilatancy, compaction, and slip instability of a fluid-infiltrated fault. *J. Geophys. Res.* **100,** 22155–22171 (1995).
12. Remitti, F., Bettelli, G. & Vannucchi, P. Internal structure and tectonic evolution of an underthrust tectonic mélange: the Sestola–Vidiciatico tectonic unit of the Northern Apennines, Italy. *Geodin. Acta* **20,** 37–51 (2007).
13. Plesi, G. *Foglio 235 Pievepelago e Note illustrative della carta geologica d'Italia alla scala 1:50.000*. (S.EL.CA., Firenze, 2002).
14. Landuzzi, A. Relationships between the Marnoso–Arenacea formation of the Inner Romagna Units and the Ligurids (Italy). *Mem. Soc. Geol. Ital.* **48,** 523–534 (1994).
15. Cibin, U., Spadafora, E., Zuffa, G. G. & Castellarin, A. Continental collision history from arenites of episutural basins in the Northern Apennines, Italy. *Geol. Soc. Am. Bull.* **113,** 4–19 (2001).
16. Amorosi, A. Miocene shallow-water deposits of the northern Apennines: A stratigraphic marker across a dominantly turbidite foreland-basin succession. *Geol. Mijnbouw* **75,** 295–307 (1996).
17. Reches, Z. Faulting of rocks in three-dimensional strain fields. II. Theoretical analysis. *Tectonophysics* **95,** 133–156 (1983).
18. Healy, D., Jones, R. R. & Holdsworth, R. E. Three-dimensional brittle shear fracturing by tensile crack interaction. *Nature* **439,** 64–67 (2006).
19. Moore, J. C. & Byrne, T. Thickening of fault zones: A mechanism of melange formation in accreting sediments. *Geology* **15,** 1040–1043 (1987).
20. Sibson, R. H. Conditions for fault-valve behaviour. *Geol. Soc. Spec. Publ.* **54,** 15–28 (1990).
21. Sibson, R. H. Implications of fault-valve behavior for rupture nucleation and recurrence. *Tectonophysics* **18,** 1031–1042 (1992).
22. Reutter, K. J., Heinitz, I. & Eusslin, R. Structural and geothermal evolution of the Modino–Cervarola Unit. *Memorie Carta Geologica d'Italia* **46,** 257–266 (1992).
23. Zattin, M., Landuzzi, A., Picotti, V. & Zuffa, G. G. Discriminating between tectonic and sedimentary burial in a foredeep succession, Northern Apennines. *J. Geol. Soc. Lond.* **157,** 629–633 (2000).
24. Obana, K. *et al.* Microseismicity at the seaward updip limit of the western Nankai Trough seismogenic zone. *J. Geophys. Res.* **108,** doi:10.1029/2002JB002370 (2003).
25. Moore, J. C. & Saffer, D. Updip limit of the seismogenic zone beneath the accretionary prism of southwest Japan: An effect of diagenetic to low-grade metamorphic processes and increasing effective stress. *Geology* **29,** 183–186 (2001).
26. Sibson, R. H. Controls on low-stress hydrofracturing dilatancy in thrust, wrench and normal fault terrains. *Nature* **289,** 665–667 (1981).
27. Bangs, N. L. B., Gulick, S. P. S. & Shipley, T. H. Seamount subduction erosion in the Nankai Trough and its potential impact on the seismogenic zone. *Geology* **34,** 701–704 (2006).
28. Harris, R. N. & Wang, K. Thermal models of the middle America trench at the Nicoya Peninsula, Costa Rica. *Geophys. Res. Lett.* **29,** doi:10.1029/2002GL015406 (2002).
29. Ranero, C. R., Weinrebe, W., Grevemeyer, I., von Huene, R. & Reichert, C. The relation between tectonics, fluid flow and seismogenesis at convergent erosional margins. *Eos Trans. AGU* 85, Fall Meet. Suppl. Abstract S43D–01 (2004).

Supplementary Information is linked to the online version of the paper at www.nature.com/nature.

Acknowledgements We thank J. P. Morgan for discussions and G. Ruggeri for sharing preliminary results on fluid inclusion analysis. This work is a contribution to PRIN 'Dynamics in subduction complexes: mass transfer in fossil systems and comparison with modern examples'.

Author Contributions All authors participated in collecting the data, interpretation of results and developing the model. P.V. wrote the paper. G.B. conceived the project.

Author Information Reprints and permissions information is available at www.nature.com/reprints. Correspondence and requests for materials should be addressed to P.V. (paola.vannucchi@unifi.it).